Archimedes Consulting Pty Ltd

Processing & Analysis of the Aeromagnetic Survey Data over part of the Otway Basin in Victoria PEP 153/154a,b

Phase I

Report

Prepared for

SANTOS LTD

Adelaide, November 2000

Archimedes Consulting Pty. Ltd.
A.B.N. 82 739 589 598
24 Stirling Street, Thebarton, SA 5031, Australia, PO Box 423, Glenside, SA 5065, Australia, Tel +61 8 8234 0511, +61 8 8303 3358, Fax:+61 8 8234 2637, Mobile: 0412 490 904, E-mail:ikivior@archimedes-consulting.com.au

TABLE OF CONTENTS

EXECUTIVE SUMMARY

The special processing, analysis and interpretation of the high-resolution magnetic data over the onshore part of the Otway Basin covered by Santos Ltd exploration permits PEP-153 and PEP-154a/b, by Archimedes Consulting Pty Ltd, has provided information which is of great assistance in the interpretation of the structure and understanding the geology in relation to CO_2 occurrences. . This project also involved the analysis and special processing of aeromagnetic data over the adjacent offshore section of the Otway Basin. This study focused on the delineation of deep-seated basement faults and structure patterns and the detection of possible CO_2 sources such as magma chambers located in the lower crust or shallower magmatic intrusions within the sedimentary section and underlying basement.

This project, which is considered as Phase-I of a more complex study, has proven that the application of new methods and techniques to the interpretation of high-resolution aeromagnetic data over sedimentary basins and the underlying deeper crust can value-add to a petroleum exploration program.

The analyses of grid data were carried out, over selected data sub-sets, by the application of specially designed anomaly separation filters derived from the energy spectra. This brought an understanding of the distribution and character of magnetic anomalies arising from magnetic sources located at depths of 2km to more than 19km.

The automatic curve matching (ACM) method was successfully applied to profiles extracted from the TMI grid in EW, NS, NW and NE directions. The ACM method allowed the detection of a very large number of magnetic sources within the shallower (2-8km) sedimentary section of the onshore and offshore Otway Basin and subsequently the detection of shallow-seated faults and, presumably, associated structure patterns. ACM detected many thousands of magnetic sources present in deeper parts of the basin and the underlying basement to depths exceeding 30km.

Results obtained from ACM were plotted as magnetic source maps (MSM) for four horizontal crustal depth bands at depths of:

- 2km to 4km; sedimentary section,
- 4km to 8km; sedimentary section,
- 8km to 18km; deepest part of the basin and the underlying pre-Jurassic basement, and
- greater than 18km (exceeding 30km); middle and lower crust.

In the analysed area, the relationship of the magnetic-source maps to the geology can be easily seen. There are two main trends of magnetic lineaments, which persist at depth. The northwest-southeast magnetic lineaments correspond to the orientation of the major basin forming faults observed on a regional scale. These magnetic lineaments reflect the characteristic structural grain of the region. However, there is also a dominant pattern of deep-seated magnetic lineaments trending in the northeast-southwest direction. In general this orientation corresponds to the axis trends of fold structures forming the Otway Ranges.

However, there are also several deep-seated magnetic lineaments trending towards the NS, which correspond to the direction of transform faults dislocating the oceanic crust. The position of some of these MLs corresponds to the position of the Woorudoo Fault Zone cross-cutting the Palaeozoic basement on the northern flank of the rift. The lower crust is also controlled by an ENE trending discontinuity. Several MLs of a similar orientation can be seen in the shallower crust. Some of these MLs correspond to surface faults.

The magnetic lineaments often represent fault zones and/or fault-associated structures. It has been confirmed in other studies, that the defined lineaments correspond to the position of faults. Often magnetic lineaments indicate the strike of fault structures and should be used by geologists as a guide in the structural interpretation of seismic data.

As the main purpose of this study was to establish the migration paths of CO_2 and detect the presence and delineate the shape and depths of possible sources of the CO_2, which, as indicated by an isotopic study, is of magmatic origin, the attention focused on the wells in which the CO_2 was encountered. There are four onshore wells

containing CO_2 within the Santos' permits ('Boggy Creek-1', 'Langley-1', 'Grumby-1' and 'Iona-1') and one offshore well which is located directly south of the 'Langley-1' well.

Several very large magnetic anomalies at depths exceeding 18km were delineated from the anomaly separation filter maps, and these could be due to igneous sources. In the offshore part, about 8km southwest of Port Campbell the long wave-length anomaly map shows a large magnetic anomaly arising from a source located at a depth greater than 18.8km. That anomaly indicates the presence of a large volume body composed of high susceptibility material, which is probably more basic in composition that the surrounding crust. That could be a large magma chamber from which a large magmatic body intruded the overlying crust (8.4km-18.8km). Above that large, strongly magnetic body, at depths of between 5.1km and 8.4km, there are two smaller sources composed of the high susceptibility material, which could be magmatic intrusions shooting from the deep-seated magma chamber detected at a depth of 18.8km. Superimposed on these, there is another much shallower magnetic body located at a depth of about 1.2km. That body is indicated by the anomaly separation maps, and is visible on the vertical cross-section showing the ACM results and the MSMs. These magnetic sources are aligned along a wide, very prominent crustal zone of NE-SW trending magnetic lineaments detected by ACM. This deep-crustal structural zone will be referred as the 'NE-SW Port Campbell Structural Corridor'. The 'NE-SW Port Campbell Structural Corridor' can be clearly identified at depths of 4km to more than 20km.

Therefore, it can be postulated that the 'NE-SW Port Campbell Structural Corridor' is a migration path for CO_2 towards the northeast from the deep-seated magma chamber or perhaps from shallower magmatic sources which intruded into the crust along that zone of weakness. At a depth of 2-4km it is clearly visible, that one of the magnetic lineaments within the 'NE-SW Port Campbell Structural Corridor' runs across the 'Langley 1' and 'Grumby 1' wells. There are several magnetic lineaments which could provide connecting paths for the 'Boggy Creek 1' and 'Iona 1' wells. However, the 'Iona 1' well could also have a supply of CO_2 gas from an igneous intrusion, located

towards the east and encountered in the 'Seaview 1' well at a depth of 950m. The anomaly separation map indicates that this igneous body is located close to 'Iona-1'.

Sets of magnetic features, which are of limited extent, and form distinct patterns that could be related to small faults or structures associated with the major fault system, have also been interpreted.

The large amount of information obtained from this study requires further input from project geologists, to fully integrate the interpretation of the thousands of detected magnetic features with models of the geological evolution of the basin.

It has been demonstrated that aeromagnetic survey data, if analysed and interpreted properly, can help to detect major crustal structural zones, large magmatic implacements even in the lower crust, as well as detect the presence of intrusions and volcanics, delineate sets of major faults and patterns of the small fault-associated structures within the basin's sediments and the underlying basement.

Detection of structure patterns providing migration paths for the CO_2 gas, may assist in selecting drilling sites and locating new prospects. The position of some of the major magnetic lineaments and possible intrusive and buried extrusives may be of a great importance in planning the location of a drilling site.

As shown in this report, the new methods and techniques, applied by Archimedes Consulting, work successfully in deep-crustal and sedimentary basin studies. The results obtained have proven that the skills and assets of Archimedes Consulting value-add to petroleum exploration. Therefore, it is recommended that it should be utilised not only within the Otway Basin permits, but also in other onshore and offshore sedimentary basins across Australia and other parts of the globe in which Santos has an exploration interest.

INTRODUCTION

This document describes the procedure and results of the special processing and analysis of high-resolution aeromagnetic field data over an area, covering a large part of the onshore and offshore Otway Basin in Victoria. The main aim of this project was to define the source and the migration paths of CO_2 gas within the region of the exploration permits PEP-153 and PEP-154a,b.

In this report, following a short geological summary, a brief description of the methods applied and a description of the magnetic data used, the results of the processing, analysis and interpretation of the gridded and located profile magnetic data are presented and discussed. Details concerning the location of the study-area are listed in Table 1 and are shown in Figure 1.

Table 1. Coordinates of the project areas.

Coordinates	
Latitude/Longitude	**Area [km x km]**
39°10'41"S-37°59'56"S 141°41'42"E-144°03'39"E	**200km x 130km**

The primary objective of this project was to process and analyse magnetic data to obtain information that demonstrates that high resolution aeromagnetic survey data may assist in detecting deep-seated crustal structures which control hydrocarbon migration and also in detecting large regional scale structures that influenced the development of the Otway Basin. The project was concerned with the detection and definition of magnetic bodies, which could indicate structural patterns within the top 2-8km of sedimentary sequences, and major structures within the underlying older rocks. Special processing of the magnetic data has allowed the detection and definition of major crustal lineaments cross-cutting the onshore and offshore part of the basin, which persist to the lower crust. The results obtained indicate structural patterns associated with tectonic movements both prior to and post-Jurassic rifting including recent Tertiary episodes.

To obtain a broad regional picture and to understand the anomaly distribution, the high-resolution onshore data set (50x50m grid) was merged with the offshore data set (100x100m grid). The merged data set was gridded using a 100m by 100m mesh. The high-resolution onshore gridded TMI data and the merged onshore/offshore gridded TMI data set were analysed using energy spectral analysis (ESA) and related filtering techniques, as well as other transformations. To achieve the best possible results and considering Santos' prime exploration interest, the geology of the region, as well as the geographic location, the project area has been sub-divided into several smaller blocks. Based on the energy spectrum for each block a different set of filters has been designed. In the main body of the report only selected examples are included, whereas all of the images are presented in Appendix A.

To determine with greater precision the position and depth of individual magnetic sources, magnetic anomalies were analysed using the automatic curve matching (ACM) method along profiles. A set of NS profiles was extracted every 50m from the onshore gridded TMI data, whereas from the merged onshore/offshore TMI grid profiles were extracted in four directions EW and NS every 100m, and NW and NE every 71m.

Several hundred thousand magnetic anomalies have been interpreted, and subsequently hundreds of thousands of magnetic bodies have been located in the top 2-30km of the crust.

The ACM results have been plotted on maps to show the depth to magnetic bodies at varying depth intervals. These maps will be referred to as magnetic-source maps (MSM). The MSM were constructed for four horizontal crustal depth slices (CDB 2-4km, CDB 4-8km, CDB 8-18km and CDB >18km) representing the shallow Tertiary and deeper Cretaceous/Jurassic sedimentary units within the basin, underlying older basement rocks and reaching to the upper parts of the lower crust.

The relationship of the magnetic lineaments interpreted from the MSM to the regional structural trend can easily be defined. The interpretation of the MSM for each of the

four CDBs was carried out at 1:250,000 scale. In the main body of this report the examples of four CDBs with a first-pass interpretation are presented in 1:250,000 scale. All of the magnetic-source maps presented in 1:1,000,000 scale are included in Appendix B, and are also supplied in digital form. The results obtained show the distribution of magnetic anomalies and the location in 3-D (in a first pass interpretation) of major crustal structures referred to as magnetic lineaments, features or magnetic boundaries. These magnetic features often represent fault zones and associated structures.

The amount of information obtained requires further input from geologists working in the Otway Basin area, to continue with the geological interpretation of the thousands of detected magnetic features.

Interaction with the geological team of Santos allowed the integration of the obtained results from this special analysis with geological information derived from seismic and well data.

The results obtained and presented in this report demonstrate that high-resolution aeromagnetic survey data can assist in exploration provided it is fully and properly utilised. The methods and techniques applied by Archimedes Consulting in the analysis and interpretation of magnetic data over the sedimentary basins produces valuable information which gives a better understanding of the geology of the permit area.

GEOLOGICAL SUMMARY

Regional Setting

The project area is a part of the Otway Basin, one of a series of Late Jurassic to mid-Cretaceous depocentres which developed along the south-eastern continental margin of Australia. The northwest-southeast trending basin straddles the South Australian and Victorian coastlines for 500km between Cape Jaffa and Cape Otway, covering an area of 120,000km^2 (~35% onshore). The Otway Basin is a part of the 'Southern Rift System', which extends for more than 4000km from the Broken Ridge in the west to the South Tasman Rise, and formed during the Jurassic-Cretaceous lithospheric extension and rifting which resulted in the continental breakup and separation of Australia and Antarctica. The exact nature of the tectonic processes, which formed this rift system, is still under dispute in the scientific literature (e.g. Etheridge et al., 1985, 1987; Willcox and Stagg, 1990; Williamson et al., 1990).

Santos' permit areas are located on the onshore northern margin of the basin in the Port Campbell Embayment in the State of Victoria.

Tectonic evolution

The tectonic evolution of the Otway Basin is concidered by Etheridge et al., (1985, 1987) to be initiated by ENE-SSW lithospheric extension during the Early Cretaceous. As a result of that extensional stress regime a sequence of ESE oriented shallow, seaward-dipping, normal extensional faults and orthogonal, steeply-dipping, transfer or accommodation faults developed.

Some authors (Williamson et al., 1996) imply that the tectonic evolution of the Great Australian Bight basins as described by Willcox and Stagg (1990) should be considered as it has implications for understanding the Otway Basin tectonic history.

In the Great Australian Bight basins, Willcox and Stagg (1990) suggest that the initial rifting between Australia and Antarctica, which led to the formation of the Otway Basin, occurred in two stages.

During the first stage, in the Late Jurassic/Early Cretaceous (~153Ma to 120Ma), the NW-SE extensional stress regime dominated the continental margin which extended by ~300km. During that stage, the Otway Basin was located within a left-lateral strike-slip stress regime.

In the second stage, in the Early Cretaceous (~120Ma to 100Ma), NNE-SSW extension caused the margin's extension by a further 120km. A system of ESE normal faults was formed. It is a system which dominates an offshore Otway Basin.

According to Williamson et al. (1990) it appears that in the western Otway Basin the early rift faults were oriented ENE. They suggest that these faults had been active possibly from the Late Jurassic or early Cretaceous, and a period of block faulting, rotation and erosion took place at about 120 Ma. Williamson et al. (1990) describe the structuring as 'onshore-basin precursor rifting', that accommodated initial crustal thinning prior to subsequent rifting and formation of the Otway Basin passive margin.

Hill et al. (1995) suggest that during the Early Cretaceous the whole Otway Basin was under a N-S extensional regime.

Regardless the early history of rift development, as Veevers et al. (1991) describe, continental break-up and seafloor spreading took place at about 96 Ma.

As a result of the above events, the onshore Otway Basin developed as a series of predominantly E-W to NW-SE oriented early Cretaceous troughs and half-grabens separated by basement highs. The offshore part of the basin forms three distinct tectonic provinces: the Crayfish Platform in the west, the Voluta Trough extending from west to east, and the Mussel Platform in the east. These three provinces, which probably existed since the beginning of the late Cretaceous, controlled sedimentation throughout the basin.

Litho-stratigraphy

The depositional history of the Otway Basin can be divided into five major phases associated with major tectonic events controlling basin development (Lavin, 1997).

- The oldest sedimentary sequence, a thick, Tithonian-Aptian (the Casterton and Crayfish Groups), is a syn-rift package deposited in elongate, fault controlled depocentres. Deposition was typical lacustrine to fluvial (Kopsen and Scholefield, 1990)
- The above sequence is unconformably overlain by the Aptian-Albian Eumerella Formation, non-marine unit with a significant amount of volcaniclastic detritus. The top of Eumerella Formation is bound by the 95 Ma unconformity.
- The Sherbrook Group is bounded by the 95 Ma and 67 Ma unconformities. This sequence consists of a largely marine to coastal plain succession, non-marine deposition towards the top of the sequence.
- The Wangerrip Group is a progradational, deltaic to marine succession which extended across the basin.
- The post mid-Eocene Nirranda and Heytesbury Groups form a progradational marine succession dominated by limestones and marls. This succession is characterised by sediments that were deposited in an open marine environment.

THE AEROMAGNETIC SURVEY DATA

The onshore part of the project area is covered by a high-resolution aeromagnetic survey flown for the Geological Survey of Victoria by the geophysical contractor, World Geoscience Corporation Ltd in January-April 1999. The survey was flown at an altitude of 80m, and contains, in total, 160,000km of flight lines. Data was collected along 200m spaced traverses oriented east-west with the controlling tie lines, being 2km apart, flown in a north-south direction. Details concerning the location and extent of the whole onshore survey area are listed in Table 1.

Table 1. Location of the aeromagnetic survey area.

Project Area	**1:100,000 Map sheets covered by the survey**	**Magnetic Data Set**
Onshore Otway Basin	Sorrento, Geelong, Otway, Mortlake, Corangamite and parts of Princetown, Port Campbell, Colac, Warrnambool, Portland, Nelson,Hamilton, Coleraine, Casterton, Ararat and Grampians	• Traverses spaced 200m; • Tie lines spaced 2km; • Altitude – 80m above ground level; • Total line kilometres – 160,000km

The offshore area adjacent to the PEP 153/154 permits is covered by a 500m line spacing aeromagnetic survey flown in 1994 by AGSO/PIRSA/NRE.

The onshore and offshore magnetic data sets have been merged together. The merged onshore and offshore data have been gridded using a 100m by 100m mesh.

The magnetic field inclination for the central part of the project area equals –70.045°; declination equals 10.68°, total field strength 61,800nT.

The high-resolution onshore TMI grid data (50mx50m) and merged onshore/offshore TMI grid data (Figure 2; 100m x 100m mesh) were especially processed and analysed (e.g. see the vertical gradient of TMI in Figure 3). To analyse single anomalies using the ACM method several sets of profiles were extracted from grid (Table 2). A set of the NS profiles was extracted every 50m from the onshore gridded TMI data, whereas from the merged onshore/offshore TMI grid profiles were extracted in four directions EW and NS every 100m, and NW and NE every 71m.

Table 2. Total length of magnetic profiles extracted from TMI grid data across project area.

Profile direction	Onshore Data Set [50x50m] Profile length [km]	Merged On/Offshore Data [100x100m] Profile length [km]	Comments
NS	200,000km	180,000km	• NS profiles were extracted every 50m from the TMI grid over the onshore part of the project area • NS profiles were extracted every 100m along the TMI grid columns across the entire area
EW		180,000km	EW magnetic profiles were extracted every 100m along the TMI grid rows across the entire area;
NE-SW		250,000km	NE-SW magnetic profiles were extracted every 71m across the entire area;
NW-SE		250,000km	NW-SW magnetic profiles were extracted every 71m across the entire area;
Total	200,000km	860,000km	• ACM was applied to analyse each single anomaly in the specified wavelength range. • Each profile was scanned several times using a different anomaly-searching window • In total over 1,000,000km of profile data was analysed using the ACM method.

METHODOLOGY

Two principal methods are used in the process of analysis and interpretation of the magnetic field:

(i) **Energy Spectral Analysis** (ESA) applied to **grid data**

(ii) **Automatic Curve Matching** (ACM) applied to the **profile data extracted from grid,** in east-west and north-south directions.

- **The principles of spectral analysis**

Energy spectral analysis provides a technique for quantitative studies of large and complex aeromagnetic data sets. The energy spectrum of magnetic data provides the characteristics of the data structure and combined information on the anomalies' parameters such as the frequencies and wavelengths involved, together with the directions and trends of the magnetisation.

The principles of the method are based on the fundamental work done by Bhattacharyya (1966). This method was further developed and tested by Spector (1968) and Spector and Grant (1970). Over the years many other scientists have contributed to the development of this method. The logarithm of the radial average of the energy spectrum (the square of the Fourier amplitude spectrum) is plotted versus the radial frequency. The slopes of linear segments of the spectrum correspond to separate depth ensembles and provide parameters used for the design of numerous filters (Figure 4a-b). The energy spectrum shown in Figure 4a is computed over 'SQ-Large', the location of which is shown in Figure A1.19.

The spectrum presented in Figure 4 shows a number of linear segments. The slope of each segment provides information about the depth to the top of an ensemble of magnetic bodies. The higher frequency end of the spectrum is dominated by the anomalies derived from shallow magnetic bodies and magnetic noise; at the low frequency end the main contributors to the energy spectrum are deep-seated magnetic bodies.

- **Automatic Curve Matching**

The automatic curve matching method (ACM) was applied to the profile data extracted from the TMI grid. The method works by identifying a magnetic anomaly on a profile and comparing the observed anomaly with one that is computed for a theoretical prism, varying the parameters and accepting the model which provides the best fit (Shi, 1993).

Analysis of magnetic anomalies along the profile has the advantage of a higher resolution of detected structures than can be obtained using the energy spectrum. One very special advantage of the method is its ability to provide good estimates of depth from data with a high noise level; in this project the 'noise' is the signal which comes from the near surface geology.

This method was applied to the profile data extracted from the TMI grid, in EW, NS, NW-SE and NE-SW directions. As the magnetic nature of the rocks varies greatly, so the magnetic data set was filtered and was analysed using several different initial models. The aim was to analyse, in several separate attempts using TMI data, as many single anomalies as possible of the specified range of wavelengths. An example of profile data with automatically computed results using the dyke model is shown in Figure 5.

ANALYSIS OF GRIDDED MAGNETIC DATA

To obtain a broad regional picture and an understanding of the anomaly distribution, both onshore and offshore, the gridded and merged TMI data was analysed using energy spectral analysis (ESA) and related filtering techniques, as well as other transformations.

In this stage of the project a several factors have been considered, such as the location of the area of prime interest, the different resolution of the onshore and offshore survey data, as well as the regional nature and also the local nature of the problem to be solved. Therefore, to achieve the best possible results in detecting deep-seated magnetic bodies presumably within the upper part of the lower crust, and also not to remove/filter or truncate magnetic anomalies on a local scale, the project area has been sub-divided into several larger and smaller blocks. Based on the energy spectrum for each block a different set of filters has been designed. In the main body of the report only selected examples are included (the Figure 6 series), whereas all of the images are presented in Appendix A.

The location of a square, the reduced-to-the-pole TMI field (RTP) and vertical gradient of RTP over each of the analysed sub-sets are shown in sets of Figures A1.1-A1.20 and A2.1-A2.20 respectively.

5.1 Major magnetic interfaces detected from the spectral analysis

Initially the energy spectrum was computed over each analysed square (Figures A3.1-A3.20). The spectra computed show a number of linear segments, indicating the position of major magnetic boundaries within the top 20km of the crust. Table 3 lists the depth values interpreted from the computed energy spectra over these blocks.

Table 3. Depths to the major magnetic boundaries detected from spectral analysis

SUB-AREA	DEPTH TO MAJOR MAGNETIC BOUNDARY*					
	OFFSHORE DATA SET 50x50m grid			ONSHORE DATA SET 100x100m grid		
	$Depth_I$	$Depth_{II}$	$Depth_{III}$	$Depth_I$	$Depth_{II}$	$Depth_{III}$
SQ1				1.3km	2.95km	7.4km
SQ2	1.9km	3.4km	10km	1.5km	3.5km	8.0km
SQ3	3.0km	3.65km	11.9km	2.2km	6.55km	10.4km
SQ4	1.3km	1.97km	13.0km	1.0km	4.5km	11.6km
SQ5	2.9km	5.2km	10.4km	2.2km	4.0km	6.2km
SQ6	3.0km	6.2km		2.15km	4.2km	8.0km
SQ7	1.7km		9.7km	2.15km	4.5km	10.5km
SQ8		4.9km	19.6km	2.0km	7.0km	10.2km
SQ9	1.95km		11.1km	1.2km	5.6km	
SQ10				1.52km	5.18km	

SUB-AREA	MERGED DATA SET 100x100m grid				
	$Depth_I$	$Depth_{II}$	$Depth_{III}$	$Depth_{IV}$	$Depth_V$
Square Large	390m	2.17km	5.0km	8.4km	18.8km
Square Small	440m	1.87km		8.9km	20.6km

*Altitude correction of 80 metres for onshore data and 130m for offshore data was applied

The depth computed from a slope of the spectrum shows an approximate average depth to the top of magnetic sources statistically modeled as one layer.

The ESA results indicate, in all of the onshore squares, in 'SQ-Large' and 'SQ-Small', and offshore SQ2, SQ4, SQ7 and SQ9, a shallow magnetic boundary at depths of 1km to 2.17km. As different tectonic provinces could be covered by these squares (shallow Palaeozoic basement towards the north of the Otway Basin's sediments), the magnetic boundaries indicated by ESA represent different geological interfaces.

In the onshore SQ1 and offshore SQ3, SQ5 and SQ6 the spectrum indicates a magnetic discontinuity at a depth of about 3km, whereas in the onshore SQ2 and offshore SQ2 and SQ3 there are magnetic boundaries at depths of approximately 3.5km.

In the onshore blocks, SQ4 to SQ7 there is an indication of magnetic boundaries at depths of about 4-4.5km.

In the onshore SQ3, SQ5, SQ9, SQ10 and the offshore SQ5, SQ6, SQ8 and also in 'SQ-Small' there are magnetic interfaces at depths of around 5km to 6.5km.

The spectra of the onshore SQ1-SQ4 and SQ6-SQ8, and the offshore SQ2-SQ5, SQ7, SQ9, and both 'SQ-Small' and 'SQ-Large' indicate magnetic discontinuities at a depth range of 7km up to 13km.

The largest of the analysed blocks show a magnetic inhomogeneity at approximately 20km. These large blocks were designed to detect the deepest magnetic sources present within the upper section of the lower crust ('SQ-Large', 'SQ-Small' and the offshore SQ-8).

The RTP field was further processed to emphasise magnetic boundaries and lineaments and to obtain a better understanding of the distribution of magnetic anomalies and the characteristics of the magnetic field in the study area.

5.2 Anomaly separation filters

Based on the energy spectrum for each block both onshore and offshore, a different set of filters has been designed. The characteristics of the energy spectral distribution, indicate several 'frequency cut-offs' for each of the analysed blocks (onshore SQ1-SQ10, see Figures A3.1-A3.10 and A4.1-A4.10 in Appendix A; offshore SQ2-SQ9, see Figures A3.11-A3.18 and A4.11-A4.18 in Appendix A; 'SQ-Small', see Figures A3.20 and A4.20 in Appendix A, and 'SQ-Large' see main report Figures 6). The low-pass filters have been used to separate the long wavelength component from the high-frequency component and surface-noise, and subsequently to separate the anomalies caused by superimposed sources from different depths.

The 'SQ-Large' images referred to as a set of Figures A*.19 in Appendix A, are only included in the main body of the report as the set of Figure 6.

Residual magnetic anomalies were also computed for each frequency cut-off. The residual field is computed from the RTP field by separation of the long wavelength anomalies. In a simplified geological/magnetic model of the earth crust, the residual fields represent the magnetic signal arising from magnetic sources distributed from surface to the spectrum-implied depth (Figures 6a-1 to 6a-5, see also Figures A3.1-A3.20 and A4.1-A4.20 in Appendix A).

A number of 'depth slice' maps were constructed for each sub-set of data based on the characteristics of the energy spectral frequency distribution. The spectrum of each analysed area indicates magnetic discontinuities at depths listed in Table 3 (Figures 4a-b and included in Appendix A, Figures A3.1-20 & A4.1-20.). Accordingly frequency bands have been computed to show magnetic anomalies arising from magnetic sources present within a narrow slice of the crust.

As is common practice, the description of the filtered magnetic data will be referred to in non-geophysical nomenclature, but in more understandable geological terms for explorers (instead of frequency bands we will use 'depth slicing', etc.).

5.2.1 Low-pass filters

The parameters that have been used to compute the long wavelength magnetic field, representing groups of anomalies arising from slices of the magnetic crust, are as follows.

- **Onshore 'SQ1' Low-pass Filters**

Three sets of the low-pass filtered magnetic field, representing the magnetic signature of causative bodies seated deeper than 1.3km, 2.95km and 7.4km, were computed. The images of the vertical gradients of the long wavelength anomalies rising from the respective layers of the crust are presented in Appendix A (Figure A5.1c to A5.1e).

- **Onshore 'SQ2' – Low-pass Filters**

Three sets of the low-pass filtered, magnetic field representing the magnetic signature of causative bodies seated deeper than 1.5km 3.5km and 8.0km, were computed. The images of the vertical gradients of the long wavelength anomalies rising from the respective layers of the crust are presented in Appendix A (see Figure A5.2c to A5.2e).

- **Onshore 'SQ3' – Low-pass Filters**

Three sets of the low-pass filtered magnetic field, representing the magnetic signature of causative bodies seated deeper than 2.2km, 6.55km and 10.4km, were computed. The images of the vertical gradients of these low-pass filters are shown in Appendix A (Figure A5.3c to A5.3e).

- **Onshore 'SQ4' – Low-pass Filters**

Three sets of the low-pass filtered magnetic field, representing the magnetic signature of causative bodies seated deeper than 1.0km, 4.5km and 11.6km, were computed. The images of the vertical gradients of the low-pass filters are presented in Appendix A (Figure A5.4c to A5.4e).

- **Onshore 'SQ5' – Low-pass Filters**

Three sets of the low-pass filtered magnetic field, representing the magnetic signature of causative bodies seated deeper than 2.2km, 4.0km and 6.2km, were computed. The images of the vertical gradients of the low-pass filters are presented in Appendix A (Figure A5.5c to A5.5e).

- **Onshore 'SQ6' – Low-pass Filters**

Three sets of the low-pass filtered magnetic field, representing the magnetic signature of causative bodies seated deeper than 2.15km, 4.2km and 8km, were computed. The images of the vertical gradients of the low-pass filters are presented in Appendix A (Figure A5.6c to A5.6e).

- **Onshore 'SQ7' – Low-pass Filters**

Three sets of the low-pass filtered magnetic field, representing the magnetic signature of causative bodies seated deeper than 2.15km, 4.5km and 10.5km, were computed. The images of the vertical gradients of the low-pass filters are presented in Appendix A (Figure A5.7c to A5.7e).

- **Onshore 'SQ8' – Low-pass Filters**

Three sets of the low-pass filtered magnetic field, representing the magnetic signature of causative bodies seated deeper than 2km, 7km and 10.2km, were computed. The images of the vertical gradients of the low-pass filters are presented in Appendix A (Figure A5.8c to A5.8e).

- **Onshore 'SQ9' – Low-pass Filters**

Two sets of the low-pass filtered magnetic field, representing the magnetic signature of causative bodies seated deeper than 1.2km and 5.6km, were computed. The images of the vertical gradients of the low-pass filters are presented in Appendix A (Figure A5.9d to A5.9e).

- **Onshore 'SQ10' – Low-pass Filters**

Two sets of the low-pass filtered magnetic field, representing the magnetic signature of causative bodies seated deeper than 1.52km and 5.18km, were computed. The images of the vertical gradients of the low-pass filters are presented in Appendix A (Figure A5.10c to A5.10d).

- **Offshore 'SQ2' – Low-pass Filters**

Two sets of the low-pass filtered, magnetic field representing the magnetic signature of causative bodies seated deeper than 3.4km and 10km, were computed. The images of the vertical gradients of the long wavelength anomalies rising from the respective layers of the crust are presented in Appendix A (Figure A5.11c to A5.11d).

- **Offshore 'SQ3' – Low-pass Filters**

Three sets of the low-pass filtered magnetic field, representing the magnetic signature of causative bodies seated deeper than 3km, 3.65km and 11.9km, were computed. The images of the vertical gradients of these low-pass filters are shown in Appendix A (Figure A5.12c to A5.12e).

- **Offshore 'SQ4' – Low-pass Filters**

Three sets of the low-pass filtered magnetic field, representing the magnetic signature of causative bodies seated deeper than 1.3km, 1.97km and 13km, were computed. The images of the vertical gradients of the low-pass filters are presented in Appendix A (Figure A5.13c to A5.13e).

- **Offshore 'SQ5' – Low-pass Filters**

Three sets of the low-pass filtered magnetic field, representing the magnetic signature of causative bodies seated deeper than 2.9km, 5.2km and 10.4km, were computed. The images of the vertical gradients of the low-pass filters are presented in Appendix A (Figure A5.14c to A5.14e).

- **Offshore 'SQ6' – Low-pass Filters**

Two sets of the low-pass filtered magnetic field, representing the magnetic signature of causative bodies seated deeper than 3km and 6.2km, were computed. The images of the vertical gradients of the low-pass filters are presented in Appendix A (Figure A5.15c to A5.15d).

- **Offshore 'SQ7' – Low-pass Filters**

Two sets of the low-pass filtered magnetic field, representing the magnetic signature of causative bodies seated deeper than 1.7km and 9.7km, were computed. The images of the vertical gradients of the low-pass filters are presented in Appendix A (Figure A5.16c to A5.16d).

- **Offshore 'SQ8' – Low-pass Filters**

Two sets of the low-pass filtered magnetic field, representing the magnetic signature of causative bodies seated deeper than 4.9km and 19.6km, were computed. The images of the vertical gradients of the low-pass filters are presented in Appendix A (Figure A5.17c to A5.17d).

- **Offshore 'SQ9' – Low-pass Filters**

Two sets of the low-pass filtered magnetic field, representing the magnetic signature of causative bodies seated deeper than 1.95km and 11.1km, were computed. The images of the vertical gradients of the low-pass filters are presented in Appendix A (Figure A5.18c to A5.18d).

- **Merged onshore/offshore 'SQ Large' – Low-pass Filters**

Five sets of the low-pass filtered magnetic field, representing the magnetic signature of causative bodies seated deeper than 390m, 2.17km, 5.0km, 8.4km and 18.8km, were computed. The images of the vertical gradients of the low-pass filters are presented as Figures 6b-1 to 6b-5.

- **Merged onshore/offshore 'SQ Small' – Low-pass Filters**

Four sets of the low-pass filtered magnetic field, representing the magnetic signature of causative bodies seated deeper than 440m, 1.87km, 8.9km and 20.6km, were computed. The images of the vertical gradients of the low-pass filters are presented in Appendix A (Figure A5.20a to A5.20d).

5.2.2 Residual fields

The low frequency component was subtracted from the original RTP field producing a short wavelength magnetic field that is referred to as the residual field. This has been computed for each of the selected frequency cut-off or the equivalent depth values indicated by the energy spectrum.

- **Onshore 'SQ1' - Residual**

The images of the residual magnetic anomaly field from the following slices of the crust: 0m-1.3km, 0m-2.95km and 0m-7.4km are included in Appendix A (Figure A6.1c to A6.1e).

- **Onshore 'SQ2' - Residual**

The images of the residual magnetic anomaly field from the following slices of the crust: 0m-1.5km, 0m-3.5km and 0m-8km are included in Appendix A (Figure A6.2c to A6.2e).

- **Onshore 'SQ3' - Residual**

The images of the residual magnetic anomaly field from the following slices of the crust: 0m-2.2km, 0m-6.55km and 0m-10.4km are included in Appendix A (Figure A6.3c to A6.3e).

- **Onshore 'SQ4' - Residual**

The images of the residual magnetic anomaly field from the following slices of the crust: 0m-1km, 0m-4.5km and 0m-11.6km are included in Appendix A (Figure A6.4c to A6.4e).

- **Onshore 'SQ5' - Residual**

The images of the residual magnetic anomaly field from the following slices of the crust: 0m-2.2km, 0m-4km and 0m-6.2km are included in Appendix A (Figure A6.5c to A6.5e).

- **Onshore 'SQ6' - Residual**

The images of the residual magnetic anomaly field from the following slices of the crust: 0m-2.2km, 0m-4.2km and 0m-8km are included in Appendix A (Figure A6.6c to A6.6e).

- **Onshore 'SQ7' - Residual**

The images of the residual magnetic anomaly field from the following slices of the crust: 0m-2.15km, 0m-4.5km and 0m-10.5km are included in Appendix A (Figure A6.7c to A6.7e).

- **Onshore 'SQ8' - Residual**

The images of the residual magnetic anomaly field from the following slices of the crust: 0m-2km, 0m-7km and 0m-10.2km are included in Appendix A (Figure A6.8c to A6.8e).

- **Onshore 'SQ9' - Residual**

The images of the residual magnetic anomaly field from the following slices of the crust: 0m-1.2km and 0m-5.6km are included in Appendix A (Figure A6.9d to A6.9e).

- **Onshore 'SQ10' - Residual**

The images of the residual magnetic anomaly field (VG) from the following slices of the crust: 0m-1.5km and 0m-5.18km are included in Appendix A (Figure A6.10c-1 to A6.10d-1).

- **Offshore 'SQ2' - Residual**

The images of the residual magnetic anomaly field (VG) from the following slices of the crust: 0m-3.4km and 0m-10km are included in Appendix A (Figure A6.11c-1 to A6.11d-1).

- **Offshore 'SQ3' - Residual**

The images of the residual magnetic anomaly field (VG) from the following slices of the crust: 0m-3km, 0m-3.65km and 0m-11.9km are included in Appendix A (Figure A6.12c-1 to A6.12e-1).

- **Offshore 'SQ4' - Residual**

The images of the residual magnetic anomaly field (VG) from the following slices of the crust: 0m-1.3km, 0m-1.97km and 0m-13km are included in Appendix A (Figure A6.13c-1 to A6.13e-1).

- **Offshore 'SQ5' - Residual**

The images of the residual magnetic anomaly field (VG) from the following slices of the crust: 0m-2.9km, 0m-5.2km and 0m-10.4km are included in Appendix A (Figure A6.14c-1 to A6.14e-1).

- **Offshore 'SQ6' - Residual**

The images of the residual magnetic anomaly field (VG) from the following slices of the crust: 0m-3km and 0m-6.2km are included in Appendix A (Figure A6.15c-1 to A6.15d-1).

- **Offshore 'SQ7' - Residual**

The images of the residual magnetic anomaly field (VG) from the following slices of the crust: 0m-1.7km and 0m-9.7km are included in Appendix A (Figure A6.16c-1 to A6.16d-1).

- **Offshore 'SQ8' - Residual**

The images of the residual magnetic anomaly field (VG) from the following slices of the crust: 0m-4.9km and 0m-19.6km are included in Appendix A (Figure A6.17c-1 to A6.17d-1).

- **Offshore 'SQ9' - Residual**

The images of the residual magnetic anomaly field (VG) from the following slices of the crust: 0m-1.95km and 0m-11.1km are included in Appendix A (Figure A6.18c-1 to A6.18d-1).

- **Merged onshore/offshore 'SQ Large' - Residual**

Five sets of images of the residual magnetic anomaly field from the following slices of the crust: 0m-390m, 0m-2.17km, 0m-5.0km, 0m-8.4km and 0m-18.8km are included as Figures 6a-1 to 6a-5.

- **Merged onshore/offshore 'SQ Small' - Residual**

Four sets of the images of the residual magnetic anomaly field from the following slices of the crust: 0m-440m, 0m-1.87km, 0m-8.9km and 0m-20.6km are included in Appendix A (Figure A6.20a to A6.20d).

5.2.3 'Depth slice' maps

The following frequency bands referred to as 'depth slice' maps were computed for two squares cut from the merged data:

- **Merged onshore/offshore 'SQ Large' – 'Depth Slice' Maps**

The images of the magnetic anomaly field arising from slices of the crust at depths of 390m to 2.17km, 2.17km to 5.0km, 5.0km to 8.4km and 8.4km to 18.8km are shown as Figures 6c-1 to 6c-4.

- **Merged onshore/offshore 'SQ Small' – 'Depth Slice' Maps**

The images of the magnetic anomaly field arising from slices of the crust at depths of 440m to 1.87km, 1.87km to 8.9km and 8.9km to 20.6km are shown in Appendix A (Figure A7.20a to A7.20c).

5.3 Summary of the analysis of magnetic grid data.

5.3.1 Magnetic Signature of the Basement

Maps showing the results of the anomaly separation, which was based on the energy spectra for selected squares (see Appendix A), are particularly useful in detecting major structural trends and the presence and orientation of magnetic sources in various sections of the magnetic crust. There are a large number of structures or magnetic boundaries, which can be seen on the low-pass filters and residual field maps and on the 'depth slice' maps. The entire set of low-pass filter maps and residual anomaly maps were analysed and interpreted. The preliminary results of this analysis were used as guidance for the interpretation of ACM results, which will be discussed in the later chapters of this report.

Figure 6b-1 shows the 'Low-pass Filter 1' map of 'SQ-Large' (depth > 340m). The high frequency component arising from depths shallower than 390m, has been removed. There is a very prominent east-west boundary at approximately 575000mE, which presumably reflects the basin's northern margin. It is also clearly visible on the images of RTP and the vertical gradient of RTP (Figures 6-1/2) that the area north of that boundary is covered by shallow, near surface volcanics. On the image of 'Low-pass Filter 2' of 'SQ-Large' (depth > 2.17km), shown in Figure 6b-2, north of that east-west boundary magnetic anomalies are visible that arise from the shallow basement. On the 'Low-pass Filter 3' map of 'SQ-Large' (depth > 5.1km; Figure 6b-3) that boundary is very prominent, the magnetic signature of rocks north of it is very different than towards the south. Thick sediments cover the area south of that boundary. The ESA of 'SQ-Large' indicates a significant magnetic inhomogeneity at a depth of approximately 8.4km. An image of 'Low-pass Filter 4' of 'SQ-Large' shown in Figure 6b-4 still indicates some difference in the magnetic anomaly pattern between the shallow basement on the northern flank of the rift and the basement underlying the basin's sediments. As indicated by a deep-seismic survey (Moore et al., 2000) conducted by AGSO across the Otway Basin, the thickness of the sediments in the vicinity of this project area (Nelson Sub-basin) appears to be about 8km (5s TWT).

5.3.2 A 3-D Model of the Magnetic Crust.

A 3-D model of the magnetic crust of the onshore and offshore Otway Basin is presented in a set of Figures 12a-12c. As the main objective of Phase I of this project was to conduct a deep-crustal study, the top 2km of the crust was not considered at all, and special attention was focused on structures located at depths greater than 4km.

The 3-D model of the magnetic crust shows, at depth, the position of the major magnetic lineaments, often representing major fault and/or shear zones as well as associated structure patterns, also an outline of high magnetic susceptibility material, such as volcanics or magmatic intrusions. In addition to the 3-D model of the deeper crust described below, a map showing outlines of possible igneous bodies located in the shallow section of the upper crust was constructed (see Figure 7- magnetic anomaly map, h< 1.5km). Several of the outlined magnetic anomalies are of a similar strong magnetic signature. However, the source of these magnetic anomalies is unknown and potentially these anomalies could be due to buried volcanic lava, tuffs or volcanic ash. It is recommended that, before drilling any wells, these anomalies be further investigated for changes of amplitude on seismic traverses, as is typical for volcanic rocks.

The 3-D picture of the crust is presented as a set of the following Horizontal Crustal 'Depth-Slices' constructed using the integrated ESA/transformations and ACM results: 2km-4km (ESA depths: 2.17km-5.1km), 4km-8km (ESA depths: 5.1km-8.4km), 8km-18km (ESA depths: 8.4km-18.8km) and the crust deeper than 18km, exceeding 30km (ESA depths >18.8km).

A number of major linear magnetic features can be seen on the low-pass and residual field maps and also the images of the vertical gradient of RTP. There are clearly visible magnetic features, such as magnetic lineaments truncating magnetic anomalies, or the axis of elongated magnetic anomalies, trending in four principal directions and propagating at depth.

- **Horizontal Crustal 'Depth-Slice' 2.17km-5.1km (ACM depths: 2km-4km)**

The dominant orientation of the magnetic features at depths greater than 2.17km and shallower than 5.1km is, in general, the NW-SE direction, reflecting the structural grain of the basin's architecture, both onshore and offshore. The 'Low-Pass Filter 2' map of 'SQ-Large' and image of 'Depth-Slice 2' shown in Figures 6b-2 & 6c-1 clearly indicate the presence of a strong NW-SW regional structural trend. There is also evidence that the anomaly patterns are truncated along NS lineaments. There are a number of features that cut across the main structures of the area. Displacement of magnetic anomalies and abrupt truncation of structures indicates the presence of faults that displace the sediments.

In the offshore part of the basin, approximately 10km southwest of Langley-1 and Grumby-1 wells a prominent magnetic anomaly outlined in Figure 8c as the 'Anomaly-A' is visible. This anomaly appears to be due to reasonably shallow magnetic sources either buried volcanics or perhaps a magmatic intrusion.

The Seaview-1 well, which intersected gabbroic material at a depth of 950m, is located on the eastern edge of the magnetic anomaly, which is presumably due to a magmatic intrusion.

- **Horizontal Crustal 'Depth-Slice' 5.1km-8.4km (ACM depths: 4km-8km)**

As visible on 'Low-Pass 3' and 'Depth-Slice 4' of 'SQ-Large' (Figures 6b-3 & 6c-3), within the area covered by the basin, the magnetic anomalies form a pattern of elongated features in NW-SE and NE-SW directions.

Southwest of 'Anomaly-A', there are two magnetic anomalies arising from magnetic sources present at depths exceeding 5.1km. It appears that these two magnetic anomalies, 'Anomaly-B' and 'Anomaly-C' as well as 'Anomaly-A' are due to magnetic bodies lying along a NE-SW trend. As indicated in Figure 9c there are several anomalies forming a similar pattern.

The basin's northern margin is very distinct as well as the NW-SE oriented lineaments cross-cutting the NE-SW trending anomalies. However, at this depth the crust is not only dominated by the NE-SW trending anomaly pattern, but also abrupt truncation of the anomalies along a NE-SW oriented lineament, which is sub-parallel to the anomaly pattern described above (see Figure 9c). This magnetic lineament appears to be reflecting large fault structure dislocating not only the Otway Basin's sediments but also basement rocks on the northern margin. That fault structure is a deep-crustal feature as it is also observed at greater depths both in crustal depth-slices 8.4km-18.8km and >18.8km, where it became a wide structural zone dipping towards the southeast.

- **Horizontal Crustal 'Depth-Slice' 8.4km-18.8km**
  (ACM depths: 8km-18km)

At depths of 8.4km to 18.8km, the region is dominated by magnetic features of a NE-SW and NW-SE orientation (see the 'Low-Pass 4' and 'Depth-Slice 5' of 'SQ-Large' in Figures 6b-4 & 6c-4). There are also N-S trending large-scale regional magnetic features that appear to be influencing the anomaly pattern both offshore and onshore (Figures 10a-c).

Along the deep-crustal structural zone, described above, cross-cutting the offshore and onshore Otway Basin as well as the basement rocks north of the basin's margin, there is a large implacement of high magnetic susceptibility material superimposed beneath the magnetic bodies causing 'Anomaly-A', 'Anomaly-B' and 'Anomaly-C' (see 'Anomaly-D' in Figure 10c).

- **Horizontal Crustal 'Depth-Slice' h>18.8km**
  (ACM depths >18km)

As visible on the 'Low-pass Filter 5' map of 'SQ-Large' (Figure 6b-5), in deeper parts of the crust at depths exceeding 19km, there is not a significant difference in the magnetic signature of the magnetic sources in the southern and the northern part of the SQ-Large area. In the southern half of the area, a very abrupt truncation of two large

magnetic anomalies along a ENE-WSW trending boundary (080°N) is visible. This boundary is perhaps connected with a NNW-SSE oriented stress regime, which dominated that part of the margin of the Australian continent in the early stages of lithospheric extension.

Several broad linear structures dominate the deep crust in this region. As indicated in Figure 6b-5, across the 'SQ-Large' area there are four large, NW-SE oriented, lineaments marking boundaries between high magnetic susceptibility material and non-magnetic rocks. The lower crust in this region is also controlled by NE-SW trending structures. These sub-parallel linear bounding-structures together with the above-mentioned NW-SE set of lineaments, sub-divide the lower crustal material into zones of non-magnetic and high magnetic susceptibility blocks.

The NE-SW trending magnetic lineament observed in the shallower parts of the crust (crustal depth-slices: 5.1km-8.4km and 8.4km-18.8km) with which 'Anomaly-A', 'Anomaly-B', 'Anomaly-C', and 'Anomaly-D' are associated, forms in this part of the lower crust, a few kilometres wide structural zone that will be referred to as the 'NE-SW Port Campbell Structural Corridor'.

The 'NE-SW Port Campbell Structural Corridor' is controlling deeper parts of the crust underlying the area covered by Santos' PEP-153 permit. This 'NE-SW Port Campbell Structural Corridor', presumably is a zone of crustal weakness, which provides a space for mantle material to intrude the lower crust. Along that crustal zone, in the southwestern part of 'SQ-Large', a large long wavelength magnetic anomaly, 'Anomaly-E', is super-imposed under the four above-mentioned anomalies, A, B, C and D. 'Anomaly-E' could be caused by a large mass of a mantle material emplaced at a depth of about 19km, along the 'NE-SW Port Campbell Structural Corridor', that is a magma chamber from which magma intruded into the overlying shallower crust. Such a magmatic system could be still connected with the mantle. As the Otway Basin region is an active volcanic province with the underlying hot spot (Foden, 2000), a magmatic system placed within the 'NE-SW Port Campbell Structural Corridor' could provide a source and migration path for CO_2 gas

encountered in several wells (the onshore Langley-1, Grumby-1, Iona-1, Boggy Creek 1, and the offshore Minerva 1) located in its vicinity.

Geological interpretation of results reported here, and integration of these with a detailed geological knowledge of the area will enhance models for the structural and geological evolution of this area. This phase of the interpretation needs to be conducted by a geologist with knowledge of local geology and results of hydrocarbon exploration. Therefore, only some interpretation of the results generated has been made at this stage.

ANALYSIS OF MAGNETIC FIELD DATA ALONG PROFILES

During the next stage of this project the automatic curve matching method (ACM) was applied to profile data extracted from the TMI grid. This method was applied to obtain higher resolution results that allowed the more precise location of large faults and smaller structures associated with them.

6.1 Data sets and initial models used for ACM

As described in Chapter 3, the high-resolution onshore TMI grid data (50m x 50m) and the offshore TMI grid data (100m x 100m mesh) were merged and specially processed and analysed. To analyse single anomalies using the ACM method several sets of profiles were extracted from grid (see Table 2 in Chapter 3). A set of the NS profiles was extracted every 50m from the onshore gridded TMI data, whereas from the merged onshore/offshore TMI grid profiles were extracted in four directions EW and NS every 100m, and NW and NE every 71m.

The aim of the ACM analysis was to interpret, in several separate attempts using TMI data, as many single anomalies as possible of a specified wavelength range. The initial parameters for ACM were designed based on the results of spectral analysis of TMI and a geological model of the basin derived from seismic and drilling.

Profile data analysis has been conducted over the entire project area, both onshore and offshore. Each profile was scanned several times using 5 different 'anomaly searching' windows, until the anomalies of the targeted wavelength were interpreted.

To obtain the most satisfactory results the observed data were processed before the ACM method was applied. Several filtering techniques were applied to remove the noise component and to remove anomalies arising from near-surface and shallow crust sources. Initial parameters of theoretical dyke models used to calculate depth estimates were designed for each computed data set.

6.2 Depth to magnetic sources

In the main body of this report selected ACM results have been presented in the form of magnetic source maps (MSM). The MSM show the position and depth of each model, simulating the real source, as colour dots (colour indicates depth, whereas the position of each dot marks the centre of an anomaly and centre of the causative body).

The MSM showing the curve matching results presented in the main body of this report are plotted at 1:250,000 scale for the entire project area. Selected maps showing combined results with a first-pass interpretation have been included. All of the generated results are included in Appendix B (sets of maps in a scale of 1:1,000,000).

The MSM were plotted as a horizontal crustal 'depth-slices' (HCDS). The HCDS were constructed, based on the results obtained from energy spectral analysis.

- Horizontal Crustal 'Depth-Slice' 2km-4km;
- Horizontal Crustal 'Depth-Slice' 4km-8km;
- Horizontal Crustal 'Depth-Slice' 8km-18km;
- Horizontal Crustal 'Depth-Slice' H>18km.

The separate sets and combined results from the analysis of the profile data are presented in a set of diagrams included in Appendix B. The list of corresponding figures for each HCDS is included in Table 3.

3. Horizontal crustal depth slice and corresponding diagrams.

HCDS Model	List of Figures	
	Report	**Appendix B**
Horizontal Crustal 'Depth-Slice' 2km-4km	8a - 8c;	B.*[1].*[2].*[3].a to B.*[1].*[2].*[3].a
Horizontal Crustal 'Depth-Slice' 4km-8km	9a - 9c	B.*[1].*[2].*[3].a to B.*[1].*[2].*[3].b
Horizontal Crustal 'Depth-Slice' 8km-18km	10a - 10c	B.*[1].*[2].*[3].a to B.*[1].*[2].*[3].c
Horizontal Crustal 'Depth-Slice' h>18km	10_1a – 10_1c	B.*[1].*[2].*[3].a to B.*[1].*[2].*[3].d

*[1] Direction of profiles; *[2] TMI or vg(TMI); *[3] ACM Model;

The ACM results are also presented in a form of a 10km wide, over 160km long, NE-SW trending 'Vertical Crustal Cross-Section' (VCC). As shown in Figure 11a/b this VCC runs across the PEP-153 permit.

6.3 Interpretation of ACM results

6.3.1 Summary

A first-pass interpretation of the ACM results for each selected horizontal crustal 'depth-slice' is presented in this report. For each of the horizontal crustal 'depth-slice' only one representative MSM (1:250,000 scale) is included in the main part of the report (Figures 8a, 9a, 10a & 10_1a). Combined results of interpretation of the MSM sets, for each horizontal crustal 'depth-slice', are presented in Figures 8b, 9b, 10b & 10_1b. As shown in Table 3 full sets of MSMs are included in Appendix B.

As already mentioned the working scale used for interpretation was 1:250,000. Examples of all four horizontal crustal 'depth-slices' ('HCDS 2km-4km', 'HCDS 4km-8km', 'HCDS 8km-18km', 'HCDS h>18km') in the working scale 1:250,000 showing the following set of maps:

- the MSM (Figures 8a, 9a, 10a and 10-1a),
- the MSM with superimposed interpretation (Figures 8b, 9b, 10b and 10-1b),
- the interpretation of ACM results integrated with the results obtained from grid analysis (Figures 8c, 9c, 10c and 10-1c),

are presented in main body of this report as enclosures.

In the final phase of the interpretation there was cooperation with Santos's technical staff in integrating the results obtained from analyses of magnetic field data, both grid and profile data, with geological information. This helped in investigating the relationship between the CO_2 occurrences in the PEP-153/154a,b permit areas and the 3-D model of the magnetic crust constructed in this study.

The interpretation of the MSMs was carried out based on the techniques developed and experience gained over the years from research projects or numerous commercial projects conducted over many onshore and offshore sedimentary basins.

The results obtained from the first-pass interpretation show the spatial distribution of

magnetic anomalies and major crustal structures referred to as magnetic features, lineaments or magnetic boundaries.

The ACM results were also useful in the detection of igneous sources. On the VCC (Figure 11a,b), which shows ACM results within the 160km long and 10km wide crustal-strip from the surface to a depth exceeding 20km, an outline of the igneous body detected in the offshore section approximately 12km southwest of Langley-1 is apparent. This is either a magmatic intrusion or buried volcanics at a depth of about 1.1km under the sea floor.

The magnetic lineaments detected within each horizontal crustal 'depth-slice' follow:

- the NW-SE structural grain due to the stress regime responsible for the formation of the Otway Basin;
- the NE-SW oriented structures, which are dominant in the region;
- the NS oriented regional-scale structures which appear to be connected with a transform fault system which developed as a result of the separation of Australia and Antarctica.

The 3-D picture of the magnetic crust is presented as a set of maps showing magnetic lineaments (ML). Each MLs map is portraying, in a planar view, major magnetic breaks and boundaries detected within the subsequent horizontal crustal 'depth-slice', starting from the very shallow top 2km-4km of the upper crust up to the upper section of the lower crust (above the Curie isotherm).

6.3.2 Horizontal Crustal 'Depth-Slice' 2km-4km

The Horizontal Crustal 'Depth-Slice' between depths of 2km to 4km will be referred to as the 'HCDS 2km-4km', and is the approximate equivalent of the crustal slice selected based on ESA depths of 2.17km-5.1km.

Figures 8b and 8c show major magnetic lineaments detected within 'HCDS 2km-4km'. There are a large number of prominent lineaments, in general oriented towards the NW-SE and NE-SW, which can be traced over a distance of several kilometres. These lineaments form distinguishable patterns of sub-parallel sets.

These two principal lineament patterns, overprinting nearly the entire analysed area both onshore and offshore, are clearly visible in Figure 8c.

- On a regional scale the azimuth for the NW-SE lineaments swings from 300°N to ~310°N with the exception of the southwestern offshore part of the basin, which is dominated by MLs oriented ~280°N.
- The NE-SW lineaments pattern, which dominates the eastern and central part of the analysed area, is oriented in general at an azimuth of 035°N-050°N.
- In the northwestern offshore part of the basin, has been defined a distinct pattern of ML oriented approximately 080°N - ~090°N. It appears that this set of lineaments is controlled by the NW-SE lineaments which could be traced over a distance exceeding 80km.
- Immediately south and southwest of the Langley-1 well, in the offshore part of the basin, there is several sub-parallel MLs also oriented at azimuths of about 080°N.
- A similar variation in the local azimuths has been defined in the southeastern onshore part of the analysed area.

At depths of 2km-4km a set of MLs trending approximately 355°N was also detected. The structures strongly effected the offshore area with isolated lineaments trending inland.

6.3.3 Horizontal Crustal 'Depth-Slice' 4km-8km

The Horizontal Crustal 'Depth-Slice' between depths of 4km to 8km will be referred to as the 'HCDS 4km-8km', and is the approximate equivalent of the crustal slice selected based on ESA depths of 5.1km-8.4km.

The MLs interpreted within the 'HCDS 4km-8km' follow a similar pattern of azimuths as the shallower structures. As the MLs represent either large fault structures or zones of structures dislocating the deeper crust, many of them can be traced over a long distance, often exceeding 60km. The MLs are more prominent than in the shallower part of the crust, however there are sub-areas where the detected lineaments are not as numerous (Figure 9b-c).

A comparison of the MLs detected within the 'HCDS 2km-4km' (green colour lineaments) and 'HCDS 4km–8km' (red colour lineaments) is presented in Figure 12a. It is apparent that:

- Some of the very prominent shallower structures only occasionally appear at depths greater than 4km. These deeper features follow the trend of the dominant shallower structures.
- At depths of 4km-8km MLs were detected which are offset to sub-parallel shallower structures detected within the 'HCDS 2km-4km'
- There are some MLs which propagate from the shallower crust to a greater depth. This perhaps reflects the presence of large crustal features at depths of 2-8km.
- Within the 'HCDS 4km-8km' new MLs were detected which appear to have associated shallower structures
- Some of the shallower structures are abruptly terminated by the MLs detected beneath a depth of 4km
- Some of the very prominent and long MLs detected within the 'HCDS 4km-8km' follow a planar extension of the shallower and less prominent structures. These can be due to deep-seated faults, which do not affect the shallower crust

- In the southwest offshore area, at depths greater than 4km the MLs oriented at approximately 320°N reflect major faults dislocating Otway Basin's sediments.
- The 'NE-SW Port Campbell Structural Corridor' detected within the 'HCDS 2km-4km' can be traced over a distance of 160km as a very distinct continuous zone of lineaments oriented 045°N.
- Towards the northwest of the 'NE-SW Port Campbell Structural Corridor' the deeper crust (4km-8km) is dominated by MLs forming a distinct pattern oriented at an azimuth of 060°N. This MLs pattern is very prominent offshore, whereas only a few of these MLs can be traced on land.
- The NS trending MLs detected within the 'HCDS 2km-4km' form, at a depth of 4km-8km, a very prominent zone approximately between 590000mE and 640000mE. Some of these lineaments form a pattern oriented approximately 355°N, whereas a few which can be continuously traced over a distance of more than 60km follow an azimuth of 005°N.

6.3.4 Horizontal Crustal 'Depth-Slice' 8km-18km

The Horizontal Crustal 'Depth-Slice' between depths of 8km to 18km will be referred to as the 'HCDS 8km-18km', and is the approximate equivalent of the crustal slice selected based on ESA depths of 8.4km-18.8km.

At depths of 8km to 18km, the region is dominated by MLs of several different orientations (Figures 10b-c). These are large-scale regional magnetic features which form distinct patterns influencing the crust, both offshore and onshore (Figures 10b-c). As was detected in the top 2km-8km of the crust the NW-SE, NE-SW and the N-S structural trends dominate the whole region. However, at depths of 8km-18km the approximately E-W trending crustal features appear to be also of a regional nature.

- The 'NE-SW Port Campbell Structural Corridor' is about 5km wide and appears to be a significant structural zone, which penetrates the upper and the middle crust. There is a number of sub-parallel MLs to this crustal zone in the close vicinity (~15km).
- There is several large MLs trending across the area at azimuths of 030°N to 035°N.
- The entire area both onshore and offshore is dominated by MLs oriented 310°N. These features reflect deep basement faults which controlled the basin's architecture.
- There are several MLs which can be traced over a distance exceeding 40km oriented approximately 080°N.
- The western part of the offshore area is dominated by very prominent MLs trending ~225°N-285°N, with a local variation up to 300°N.

In Figure 12b MLs detected at depths of 8km-18km are shown in blue on which are superimposed MLs (shown in red) detected within the overlying 4km of the crust. The MLs marked in blue are more distinct than those shallower (marked in red) as they often reflect large, very wide fault or shear zones, or other broad crustal features.

6.3.5 Horizontal Crustal 'Depth-Slice' h>18km

This Horizontal Crustal 'Depth-Slice' represents crust deeper than 18km, and it will be referred to as the 'HCDS h>18km'. The 'HCDS h>18km' is the approximate equivalent of the crustal slice selected based on ESA depths of greater than 18.8km.

The magnetic boundaries observed at depths greater than 18km indicate differences in the lower crustal material. There are large crustal blocks, bounded by NW-SE (~310°N) and NE-SW (045°N-050°N with some MLs swinging towards the north at an azimuth of 030°N) oriented broad crustal lineaments, which contain either high magnetic susceptibility material, or they are magnetically quiet zones (Figure 10_1b – Figure 10_1c).

The 'NE-SW Port Campbell Structural Corridor' continues into the lower crust as a very distinct, more than 10km wide, zone marked by large MLs which can be traced over a distance of more than 100km.

It appears that, in this area, the lower crust and possibly the top section of the mantle beneath the Moho discontinuity was affected in the past tectonic history by the regional-scale stress regime, which generated a large, 080°N oriented discontinuity. This discontinuity is of the same orientation as the early rift ENE faults present in the western Otway Basin and reported by Williamson et al. (1990) to be active from the Late Jurassic or Early Cretaceous. Williamson et al. (1990) refers to that period of block faulting and rotation followed by erosion as 'onshore-basin precursor rifting', that accommodated initial crustal thinning prior to subsequent rifting and formation of the Otway Basin passive margin.

In the western part of the study area, the lower crust is also strongly affected by the NS trending features. As already discussed, this demonstrates that the stress regime responsible for the origin of the transform faults also affected the continental crust. The position of one of the NS trending ML corresponds to the surface expression of the Woorndoo Fault Zone dislocating the Palaeozoic basement.

Figure 12c presents in blue the MLs detected at depths of 8km-18km and, in magenta, the magnetic discontinuities observed in the lower crust at depths greater than 18km. The major ENE discontinuity present in the deeper crust has an imprint in shallower parts of the crust. At depths of 8km-18km there are several MLs oriented approximately 080°N which are either directly connected with that large discontinuity detected in the deeper crust or they are dislocating the crust along a broad zone of 20-25km north or south.

Conclusions

The unique analysis and interpretation of high resolution magnetic data over the onshore and offshore Victorian part of the Otway Basin has produced results and information which may be of great assistance in understanding the geology and structure of the project area.

This project, which is considered a Phase-I, has proven that the application of new methods and techniques to the interpretation of high-resolution aeromagnetic data can value-add to a petroleum exploration and development program. As demonstrated in this study, techniques applied by Archimedes Consulting to achieve this end consist of the special analysis of located data after initial processing and interpretation of TMI grid data. This involved two principal methods:

- energy spectral analysis and related transformations applied to **grid data**

and

- automatic curve matching method applied to **profile data**.

The onshore and offshore data sets have been merged into a uniform 100x100m TMI grid. The analyses of **grid data** were carried out by the application of special anomaly separation filters derived from the energy spectra of selected sub-sets of the magnetic data.

The analysed sub-sets of TMI data were selected from the onshore and offshore part of the area with special attention to the location of the four wells in which CO_2 has been encountered within the PEP-153/154a,b permits.

This stage brought an understanding of the distribution and character of magnetic anomalies arising from the shallow Palaeozoic basement, exposed to the north, and the several kilometre thick Otway Basin sedimentary section overlying the Pre-Jurassic basement and also from deeper parts of the crust.

The automatic curve matching method was successfully applied to **located data** along profiles extracted from TMI grid in NS, EW, NW-SE and NE-SW directions. As reported, the application of the ACM method, conducted in several separate stages,

allowed the detection of very large numbers of shallow magnetic sources (the low frequency component was filtered out) from the high frequency anomalies. This approach was very useful in the detection of shallow-seated faults and, within the top 2km-8km of sediments. To compute depth to the magnetic sources present in deeper parts of the basin, the high frequency component of the magnetic anomalies was stripped off from the profile data. This allowed the modeling of medium and long wavelength anomalies arising from the deeper sedimentary section and the underlying basement to depths exceeding 18km and even reaching 30km.

The results obtained from ACM (many thousands of magnetic sources) were plotted as magnetic source maps (MSM) for four horizontal crustal 'depth-slices': 2km-4km, 4km-8km, 8km-18km and h>18km. The ACM results were also presented in a form of a 10km wide, over 160km long, NE-SW trending 'Vertical Crustal Cross-Section' (VCC). This VCC runs across the PEP-153 permit.

The magnetic lineaments often represent fault zones and/or fault-associated structures. The large amount of information obtained from this study requires more input from geologists working in the project area who should carry on the geological interpretation of the thousands of detected magnetic features. There are a number of conclusions, which could be drawn from this study.

i. Magnetic sources occur between the top 2km and a depth of about 20km. This indicates that not only the basement is magnetic, but also there is magnetic material within the sedimentary section and consideration should be given to the possibility that this can provide additional information for understanding the occurrence of hydrocarbons within the area.

ii. It is not always known what rocks or what minerals are responsible for these anomalies. They may be:
   - volcanics
   - igneous bodies
   - sediments such as sands, or siltstones which sometimes contain magnetic

minerals (magnetite or pyrrhotite)

- magnetic minerals which have been deposited in shear or fault zones by percolating fluids.

iii. If the sources of the anomalies are magnetic sediments this may have implications for the sedimentological development of this area.

iv. If the sources are in fault zones, the presence or absence of magnetic minerals that cause anomalies which can be related to faults may indicate whether the structures have been open or closed to percolating fluids.

v. The results obtained from the analysis of grid data (ESA and related filters) show major structural features which can be traced into a deeper section of the crust. There are clearly visible major crustal trends. These magnetic trends correspond to the regional structural grain.

vi. Several magnetic anomalies at depths of about 1.5km were delineated from the anomaly separation maps, and could be due to igneous sources.

vii. The analysis of the profile data (ACM) provides a large amount of detailed information concerning the structures dislocating the Otway Basin's sediments, the underlying basement, and also the deeper crust.

viii. A 3-D model of the magnetic crust has been constructed. Several sets of magnetic lineaments have been interpreted within four, horizontal crustal 'depth-slices' representing depths of 2km-4km, 4km-8km, 8km-18km and greater than 18km.

ix. The magnetic lineament patterns potentially represent fault systems, as all of the lineaments were marked by obvious breaks in the pattern of the detected magnetic sources.

x. Sets of magnetic features, which are of limited extent, and form distinct patterns

that could be related to small faults or, alternatively, structures associated with the major fault systems, have also been interpreted. Often the large-scale faults penetrating the deeper crust show such an association with shallower structures.

xi. The change of an azimuth-pattern of magnetic lineaments could be an indication of the local stress field responsible for the origin of structures with which magnetic lineaments are associated;

xii. It appears that the main direction of magnetic lineaments, which persists at depth, is of a NW-SE and NE-SW orientation.

- The NW-SE orientation corresponds to the characteristic pattern of basin forming faults.
- The NE-SW trend follows a regional pattern such as the Otway Ranges.

xiii. A very prominent zone of MLs, a few kilometres wide, referred to (in this report) as the 'NE-SW Port Campbell Structural Corridor' can be followed from a shallow depth to the lower crust. This structural zone of crustal weakness can be traced across the entire area, both onshore and offshore over a distance of more then 160km along an azimuth of 045°N -050°N. The 'NE-SW Port Campbell Structural Corridor' runs across the PEP-153 permit.

xiv. Two of the wells: Langley-1 and Grumby-1, in which CO_2 have been encountered, has been drilled within the 'NE-SW Port Campbell Structural Corridor'. Two other onshore wells: Boggy Creek-1 and Iona-1, as well as the offshore Minerva-1 well in which CO_2 has been encountered are also in close vicinity to the 'NE-SW Port Campbell Structural Corridor'.

xv. On the VCC, which shows the ACM results within the 160km long and 10km wide crustal-strip from the surface to a depth exceeding 20km, an outline of the igneous body detected in the offshore section approximately 12km southwest of Langley-1 is apparent. This is either a magmatic intrusion or buried volcanics at a depth of about 1.1km under the sea floor.

xvi. However, there are also several deep-seated magnetic lineaments trending towards the NS, which correspond to the direction of transform faults dislocating the oceanic crust. The position of some of these MLs corresponds to the position of the Woorudoo Fault Zone cross-cutting the Palaeozoic basement on the northern flank of the rift.

xvii. The lower crust is controlled by a ENE trending discontinuity. Several MLs of a similar orientation can be seen in the shallower crust. Some of these MLs correspond to surface faults.

xviii. As the main purpose of this study was to establish the migration paths of CO_2 and detect the presence and delineate the shape and depths of possible sources of the CO_2 , all of the results, findings and observations obtained from TMI grid and profile data analysis, were considered and the following crustal model explaining the above has been constructed:

- Several very large magnetic anomalies at depths exceeding 18.8km were delineated from the anomaly separation filters maps, and these could be due to igneous sources. In the offshore part, about 8.4km southwest of the Port Campbell the long wave-length anomaly map shows a large magnetic anomaly arising from a source located at a depth greater than 18.8km. That anomaly indicates the presence of a large volume body composed of high susceptibility material, which is probably more basic in composition that the surrounding crust. That could be a large magma chamber from which a large magmatic body intruded the overlying crust (8.4km-18.8km). Above that large, strongly magnetic body, at depths between 5.1km and 8.4km, there are two smaller sources composed of high susceptibility material, which could be magmatic intrusions shooting from the deep-seated magma chamber detected at depth of 18.8km. Superimposed on these, there is another much shallower magnetic body located at depth of about 1.2km. That body is indicated by the anomaly separation maps, and is visible on the vertical cross-section showing the ACM results and the MSMs.
- These magnetic sources are aligned along a wide, very prominent crustal zone

of NE-SW trending magnetic lineaments detected by ACM. This deep-crustal structural zone has been referred to as the 'NE-SW Port Campbell Structural Corridor'. The 'NE-SW Port Campbell Structural Corridor' can be clearly identified at depths of 4km to more than 20km.

- Therefore, it can be postulated that the 'NE-SW Port Campbell Structural Corridor' is a migration path for CO_2 towards the northeast from a deep-seated magma chamber or perhaps from shallower magmatic sources which intruded into the crust along that zone of weakness.
- At a depth of 2-4km it is clearly visible, that one of the magnetic lineaments within the 'NE-SW Port Campbell Structural Corridor' runs across the 'Langley-1' and 'Grumby-1' wells. There are several magnetic lineaments, which could provide connecting paths for the 'Boggy Creek-1', and 'Iona-1' wells. However, the 'Iona-1' well could also have a supply of CO_2 gas from an igneous intrusion, located towards the east and encountered in the 'Seaview 1' well at a depth of 950m. The anomaly separation map indicates that this igneous body is located very close to 'Iona-1'.

xiv. Detection of structure patterns providing migration paths for the CO_2 gas, may assist in selecting drilling sites and locating new prospects. The position of some of the major magnetic lineaments and possible intrusive and buried extrusives may be of a great importance in planning the location of a drilling site.

Recommendations

Recommendations for further work in the Otway Basin are as follows:

i. The special processing and Archimedes' unique analysis and interpretation of magnetic data should be applied to Phase-II, which will focus on the shallow sedimentary section (top 4km) within the PEP-153/154a,b permits and their vicinity.

- This will help to detect the sets of major faults and patterns of the small fault-associated structures and perhaps fracture patterns within different stratigraphic units. Detection of local structure patterns may assist in locating new wells.

- It will also assist in the detection of sills and volcanics emplaced within the shallow sedimentary section

ii. Down-hole susceptibility logs should be carried out in all of the wells planned to be drilled in the project area.

iii. Susceptibility measurements should be taken from all cores and cuttings that are available from the major formations intersected by the wells already drilled. Magnetic susceptibility should be correlated with litho-stratigraphy to establish the magnetic signature of different geological units, and to understand and constrain the magnetic model of the sedimentary section. This, along with the results from automatic curve matching, will allow a more accurate interpolation of structures between widely spaced seismic profiles.

iv. As shown in this report, the new methods and techniques, applied by Archimedes Consulting, work successfully in sedimentary basins. These methods have made possible, the detection of a large number of magnetic sources. Subsequently it was possible to construct a 3-dimensional model of the magnetic crust showing not only major regional-scale deep crustal structures but also detect fault patterns within the sedimentary section and the underlying basement. The methods applied also allowed the delineation of the position of major igneous

bodies and relate their presence together with the major NE-SW crustal zones to CO_2 occurrences in the area.

v. It is strongly recommended to utilise the skills and assets of Archimedes Consulting not only in the Otway Basin exploration permits, but also in other onshore and offshore sedimentary basins across Australia and other parts of the globe in which Santos has an exploration interest.

References

Bhattacharyya, B.K., 1966—Continuous spectrum of the total magnetic field anomaly due to a rectangular prismatic body, *Geophysics,* 31: 96-121.

Etheridge, M.A., Branson, J.C. and Stuart-Smith, P.G., 1985, Extensional basin-forming structures in Bass Strait and their importance for hydrocarbon exploration, APEA Journal, 25: 344-361.

Etheridge, M.A., Branson, J.C. and Stuart-Smith, P.G., 1987, The Bass, Gippsland and Otway Basins, southeast Australia: a branched rift system formed by continental extension, *In* C. Beaumount and a.j. Tankard (eds). Sedimentary basins and basin-forming mechanisms, Canadian Society of Petroleum Geologists Memoir 12: 147-162.

Foden, J., Song, S.H., Smith, P.B. and Van der Steldf, B., 2000, Geochemical evolution of lithospheric mantle beneath S.E. South Australia, Chemical Geology (in press).

Hill, K.A., Finlayson, D.M., Hill, K.C. and Cooper, G.T., 1995, Mesozoic tectonics of the Otway Basin region: the legacy of Gondwana and active Pacific Margin, *APEA Journal,* 35: 467-493.

Kivior, I., 1996, A geophysical study of the structure and crustal environment of the Polda rift, South Australia, *Ph.D. thesis, Department of Geology and Geophysics, The University of Adelaide.*

Kivior, I., Boyd, D., Shi, Z. and McClay, K.R., 1993, Crustal studies of South Australia based on energy spectral analysis of regional magnetic data, *Exploration Geophysics,* 24: 603-608.

Kopsen, E. and Scholefield, T., 1990, Prospectivity of the Otway Supergroup in the central and western Otway Basin, *APEA Journal,* 35: 538-557.

Lavin, C.J., 1997, .The Maastrichtian breakup of the Otway Basin margin – a model developed by integrating seismic interpretation, sequence stratigraphy and thermochronological studies, *Exploration Geophysics,* 28 (1/2): 252-259.

Moore, A.M.G, Stagg, H.M.J. and Norvick, M.S., 2000, Deep-water Otway Basin: a new assestment of the tectonics and hydrocarbon prospectivity, *The APPEA Journal,* 40 (1): 66-84.

Shi, Z., 1993, Automatic interpretation of potential field data applied to the study of overburden thickness and deep crustal structure, South Australia, *Ph.D. thesis, Department of Geology and Geophysics, The University of Adelaide.*

Spector, A., 1968—Spectral analysis of aeromagnetic data. *PhD thesis, Department of Physics, University of Toronto, Canada, unpublished.*

Spector, A. and Grant, F.S., 1970—Statistical models for interpreting aeromagnetic data, *Geophysics,* 35: 293-302.

Veevers, J.J., Powell, C.McA. and Roots, S.R., 1991, Review of seafloor spreading around Australia. I. Synthesis of the patterns of spreading, *Australian Journal of Earth Sciences,* 38: 391-408.

Willcox, J.B. and Stagg, H.M.J., 1990, Australia's southern margin: a product of oblique extension, *Tectonophysics*, 173: 269-281.

Williamson, P.E., Swift, M.G., O'Brien, G.W. and Falvey, D.A., 1990, Two-stage Early Cretaceous rifting of the Otway Basin margin of southeastern Australia: implications for rifting of the Australian southern margin, *Geology*, 18: 75-78.

List of figures

Figure 1 OTWAY BASIN, Merged: Location of Study Area

Location of Wells [dots], Permit boundaries [dashed], Pipelines [green] & Coastline [blue]

Figure 2 OTWAY BASIN: Merged; ACM Area: 'Total Magnetic Intensity' Permit Boundaries [dashed], Wells [dots], Coastline [blue] & Pipelines [green]

Figure 3 OTWAY BASIN: Merged; ACM Area: 'Vertical Gradient' Permit Boundaries [dashed], Wells [dots], Coastline [blue] & Pipelines [green]

Figure 4a Otway Basin, Merged TMI Data: SQ-Large, Logarithmic Radial Energy Spectrum

Figure 4b Otway Basin, SQ-Large, Depth Slice Schematic

Figure 5 Example of Automatic Curve Matching

Figure 6-1 OTWAY BASIN: Merged; 'RTP'
SQ_Large: 100x100m grid
Wells, Permit Boundaries [dashed], Pipelines [green] & Coastline [blue] shown

Figure 6-2 OTWAY BASIN: Merged; 'Vertical Gradient of RTP'
SQ_Large: 100x100m grid
Wells, Permit Boundaries [dashed], Pipelines [green] & Coastline [blue] shown

Figure 6a-1 OTWAY BASIN: Merged; 'Residual 1'
SQ_Large: Depth < 390m
Wells, Permit Boundaries [dashed], Pipelines [green] & Coastline [blue] shown

Figure 6a-2 OTWAY BASIN: Merged; 'Residual 2'
SQ_Large: Depth < 2.17 km
Wells, Permit Boundaries [dashed], Pipelines [green] & Coastline [blue] shown

Figure 6a-3 OTWAY BASIN: Merged; 'Residual 3'
SQ_Large: Depth < 5.1 km
Wells, Permit Boundaries [dashed], Pipelines [green] & Coastline [blue] shown

Figure 6a-4 OTWAY BASIN: Merged; 'Residual 4'
SQ_Large: Depth < 8.4 km
Wells, Permit Boundaries [dashed], Pipelines [green] & Coastline [blue] shown

Figure 6a-5 OTWAY BASIN: Merged; 'Residual 5'
SQ_Large: Depth < 18.8 km
Wells, Permit Boundaries [dashed], Pipelines [green] & Coastline [blue] shown

Figure 6b-1 OTWAY BASIN: Merged; 'Lowpass Filter 1 [VG]'
SQ_Large: Depth > 390m
Wells, Permit Boundaries [dashed], Pipelines [green] & Coastline [blue] shown

Figure 6b-2 OTWAY BASIN: Merged; 'Lowpass Filter 2 [VG]'
SQ_Large: Depth > 2.17 km
Wells, Permit Boundaries [dashed], Pipelines [green] & Coastline [blue] shown

Figure 6b-3 OTWAY BASIN: Merged; 'Lowpass Filter 3 [VG]'
SQ_Large: Depth > 5.1 km
Wells, Permit Boundaries [dashed], Pipelines [green] & Coastline [blue] shown

Figure 6b-4 OTWAY BASIN: Merged; 'Lowpass Filter 4 [VG]'
SQ_Large: Depth > 8.4 km
Wells, Permit Boundaries [dashed], Pipelines [green] & Coastline [blue] shown

Figure 6b-5 OTWAY BASIN: Merged; 'Lowpass Filter 5 [VG]'
SQ_Large: Depth > 18.8 km
Wells, Permit Boundaries [dashed], Pipelines [green] & Coastline [blue] shown

Figure 6c-1 OTWAY BASIN: Merged; 'Depth Slice 2 [VG]'
SQ_Large: Depth, 390m to 2.17 km
Wells, Permit Boundaries [dashed], Pipelines [green] & Coastline [blue] shown

Figure 6c-2 OTWAY BASIN: Merged; 'Depth Slice 3 [VG]'
SQ_Large: Depth, 2.17 to 5.1 km
Wells, Permit Boundaries [dashed], Pipelines [green] & Coastline [blue] shown

Figure 6c-3 OTWAY BASIN: Merged; 'Depth Slice 4 [VG]'
SQ_Large: Depth, 5.1 to 8.4 km
Wells, Permit Boundaries [dashed], Pipelines [green] & Coastline [blue] shown

Figure 6c-4 OTWAY BASIN: Merged; 'Depth Slice 5 [VG]'
SQ_Large: Depth, 8.4 to 18.8 km. Wells, Permit Boundaries [dashed], Pipelines [green] & Coastline [blue] shown

Figure 7 OTWAY BASIN, Merged: Location of possible igneous bodies
delineated from filtered grid data
Anomalies generated by magnetic sources at depths of greater than 1.5 km
Wells [dots], Permit Boundaries [dashed], Pipelines [green] &
Coastline [blue] shown

Figure 8a OTWAY BASIN, Merged: All TMI; 'Depth, 2-4 km', dk-all
Depth to magnetic sources computed using ACM method.
Dot indicates source location. All TMI; dk-all: Depth, 2000-4000m
Wells, Permit Boundaries [dashed], Pipelines [green] &
Coastline [blue] shown

Figure 8b OTWAY BASIN, Merged: ALL TMI; 'Depth, 2-4 km', dk-all
Depth to magnetic sources computed using ACM method.
Interpreted lineaments from ACM analysis
Wells, Permit Boundaries [dashed], Pipelines [green] &
Coastline [blue] shown

Figure 8c OTWAY BASIN, Merged: ALL TMI; 'Depth, 2-4 km', dk-all
Magnetic lineaments and possible igneous bodies interpreted
from ACM and grid analysis
Magnetic lineaments interpreted from ACM analysis [solid black lines]
Depth, 2000-4000m: Possible volcanic bodies [Anomaly A, yellow]
Wells, Permit Boundaries [dashed], Pipelines [green] &
Coastline [blue] shown

Figure 9a OTWAY BASIN, Onshore plus Merged: ALL TMI; 'Depth, 4-8 km', dk-all
Depth to magnetic sources computed using ACM method.
Dot indicates source location. All TMI; dk-all: Depth, 4000-8000m
Wells, Permit Boundaries [dashed], Pipelines [green] &
Coastline [blue] shown

Figure 9b OTWAY BASIN, Onshore plus Merged: ALL TMI; 'Depth, 4-8 km', dk-all
Depth to magnetic sources computed using ACM method.
Interpreted lineaments from ACM analysis
Dot indicates source location. All TMI; dk-all: Depth, 4000-8000m
Wells, Permit Boundaries [dashed], Pipelines [green] &
Coastline [blue] shown

Figure 9c OTWAY BASIN, Onshore plus Merged: ALL TMI; 'Depth, 4-8 km', dk-all
Magnetic lineaments and possible igneous bodies interpreted
from ACM and grid analysis
Magnetic lineaments interpreted from ACM analysis [solid black lines]
Depth, 4000-8000m: Possible igneous bodies [pink] and
possible intrusives [Anomalies B & C, yellow]
Wells, Permit Boundaries [dashed], Pipelines [green] &
Coastline [blue] shown

Figure 10a OTWAY BASIN, Onshore plus Merged: TMI; 'Depth, 8-18 km', dk-all
Depth to magnetic sources computed using ACM method.
Dot indicates source location. All TMI; dk-all: Depth, 8000-18000m
Wells, Permit Boundaries [dashed], Pipelines [green] &
Coastline [blue] shown

Figure 10b OTWAY BASIN, Onshore plus Merged: TMI; 'Depth, 8-18 km', dk-all
Depth to magnetic sources computed using ACM method.
Interpreted lineaments from ACM analysis [red] and
grid analysis [blue]
Dot indicates source location. All TMI; dk-all: Depth, 8000-18000m
Wells, Permit Boundaries [dashed], Pipelines [green] &
Coastline [dark blue] shown

Figure 10c OTWAY BASIN, Onshore plus Merged: TMI; 'Depth, 8-18 km', dk-all
Magnetic lineaments and possible igneous bodies interpreted
from ACM and grid analysis
Magnetic lineaments interpreted from ACM [red] and
grid [blue] analysis
Depth, 8000-18000m: Possible igneous [pink] and
intrusive bodies [Anomaly D, yellow] interpreted from grid data
Wells, Permit Boundaries [dashed], Pipelines [green] &
Coastline [dark blue] shown

Figure 10_1a OTWAY BASIN, Onshore plus Merged: TMI; 'Depth, > 18 km', dk-all
Depth to magnetic sources computed using ACM method.
Dot indicates source location. All TMI; dk-all: Depth, 18000-44000m
Wells, Permit Boundaries [dashed], Pipelines [green] &
Coastline [blue] shown

Figure 10_1b OTWAY BASIN, Onshore plus Merged: TMI; 'Depth, > 18 km', dk-all
Depth to magnetic sources computed using ACM method.
Interpreted lineaments from ACM analysis
Dot indicates source location. All TMI; dk-all: Depth, 18000-44000m
Wells, Permit Boundaries [dashed], Pipelines [green] &
Coastline [blue] shown

Figure 10_1c OTWAY BASIN, Onshore plus Merged: TMI; 'Depth, > 18 km', dk-all
Magnetic lineaments and possible igneous bodies interpreted
from ACM and grid analysis
Magnetic lineaments interpreted from ACM analysis
[solid or dashed black lines]
Depth, 18000-44000m: Possible igneous bodies [pink] and possible
magma chamber or mantle source [Anomaly E, yellow]
Wells, Permit Boundaries [dashed], Pipelines [green] &
Coastline [blue] shown

Figure 11a OTWAY BASIN: Merged Data; Cross-section through Offshore section & PEP 153
Cross-section across ACM area through PEP 153
10 km wide band oriented at 40 deg. about origin [650000mE,5700000mN]

Figure 11b OTWAY BASIN: Merged Data; Cross-section through Offshore section & PEP 153
Cross-section across ACM area through PEP 153
10 km wide band oriented at 40 deg. about origin [650000mE,5700000mN]
Interpreted Magnetic Features shown in red
Position of possible intrusives outlined in orange

Figure 12a OTWAY BASIN, Merged: ALL TMI; 'Depth, 2-8 km', dk-all
Magnetic lineaments interpreted from ACM analysis
[2-4km = green, 4-8km = red]
Depth, 2000-8000m: Possible igneous bodies
[pink, Anomalies A, B & C, yellow]
Wells, Permit Boundaries [dashed], Pipelines [dark green] &
Coastline [blue] shown

Figure 12b OTWAY BASIN, Onshore plus Merged: TMI; 'Depth, 4-18 km', dk-all
Magnetic lineaments interpreted from ACM analysis
[4-8km = red, 8-18km = blue]
Depth, 4000-18000m: Possible igneous bodies
[pink, Anomalies B, C & D, yellow]
Wells, Permit Boundaries [dashed], Pipelines [green] &
Coastline [dark blue] shown

Figure 12c OTWAY BASIN, Onshore plus Merged: ALL TMI; 'Depth, > 8 km', dk-all
Magnetic lineaments interpreted from ACM analysis
[8-18km = blue, > 18km = magenta]
Depth, 8000-44000m: Possible igneous bodies
[pink, Anomaly D & E, yellow]
Wells, Permit Boundaries [dashed], Pipelines [green] &
Coastline [dark blue] shown

Figure A1.19 OTWAY BASIN: Merged: ACM Area: 'TMI'. Location of 'SQ-Large'.

Appendix A: List of Figures

SQ-1 Onshore

FigureA1.1
FigureA2.1a FigureA2.1b
FigureA3.1 FigureA4.1
FigureA5.1c FigureA5.1d FigureA5.1e
FigureA6.1c FigureA6.1d FigureA6.1e

SQ-2 Onshore

FigureA1.2
FigureA2.2a FigureA2.2b
FigureA3.2 FigureA4.2
FigureA5.2c FigureA5.2d FigureA5.2e
FigureA6.2c FigureA6.2d FigureA6.2e

SQ-3 Onshore

FigureA1.3
FigureA2.3a FigureA2.3b
FigureA3.3 FigureA4.3
FigureA5.3c FigureA5.3d FigureA5.3e
FigureA6.3c FigureA6.3d FigureA6.3e

SQ-4 Onshore

FigureA1.4
FigureA2.4a FigureA2.4b
FigureA3.4 FigureA4.4
FigureA5.4c FigureA5.4d FigureA5.4e
FigureA6.4c FigureA6.4d FigureA6.4e

SQ-5 Onshore

FigureA1.5
FigureA2.5a FigureA2.5b
FigureA3.5 FigureA4.5
FigureA5.5c FigureA5.5d FigureA5.5e
FigureA6.5c FigureA6.5d FigureA6.5e

SQ-6 Onshore

FigureA1.6
FigureA2.6a FigureA2.6b
FigureA3.6 FigureA4.6
FigureA5.6c FigureA5.6d FigureA5.6e
FigureA6.6c FigureA6.6d FigureA6.6e

SQ-7 Onshore

FigureA1.7
FigureA2.7a FigureA2.7b
FigureA3.7 FigureA4.7
FigureA5.7c FigureA5.7d FigureA5.7e
FigureA6.7c FigureA6.7d FigureA6.7e

SQ-8 Onshore

FigureA1.8		
FigureA2.8a	FigureA2.8b	
FigureA3.8	FigureA4.8	
FigureA5.8c	FigureA5.8d	FigureA5.8e
FigureA6.8c	FigureA6.8d	FigureA6.8e

SQ-9 Onshore

FigureA1.9		
FigureA2.9a	FigureA2.9b	
FigureA3.9	FigureA4.9	
FigureA5.9d	FigureA5.9e	
FigureA6.9d	FigureA6.9e	

SQ-10 Onshore

FigureA1.10		
FigureA2.10a	FigureA2.10b	
FigureA3.10	FigureA4.10	
FigureA5.10c	FigureA5.10d	
FigureA6.10c-1	FigureA6.10d-1	

SQ-2 Offshore

FigureA1.11		
FigureA2.11a	FigureA2.11b	
FigureA3.11	FigureA4.11	
FigureA5.11c	FigureA5.11d	
FigureA6.11c-1	FigureA6.11d-1	

SQ-3 Offshore

FigureA1.12		
FigureA2.12a	FigureA2.12b	
FigureA3.12	FigureA4.12	
FigureA5.12c	FigureA5.12d	FigureA5.12e
FigureA6.12c-1	FigureA6.12d-1	FigureA6.12e-1

SQ-4 Offshore

FigureA1.13		
FigureA2.13a	FigureA2.13b	
FigureA3.13	FigureA4.13	
FigureA5.13c	FigureA5.13d	FigureA5.13e
FigureA6.13c-1	FigureA6.13d-1	FigureA6.13e-1

SQ-5 Offshore

FigureA1.14		
FigureA2.14a	FigureA2.14b	
FigureA3.14	FigureA4.14	
FigureA5.14c	FigureA5.14d	FigureA5.14e
FigureA6.14c-1	FigureA6.14d-1	FigureA6.14e-1

SQ-6 Offshore

FigureA1.15
FigureA2.15a FigureA2.15b
FigureA3.15 FigureA4.15
FigureA5.15c FigureA5.15d
FigureA6.15c-1 FigureA6.15d-1

SQ-7 Offshore

FigureA1.16
FigureA2.16a FigureA2.16b
FigureA3.16 FigureA4.16
FigureA5.16c FigureA5.16d
FigureA6.16c-1 FigureA6.16d-1

SQ-8 Offshore

FigureA1.17
FigureA2.17a FigureA2.17b
FigureA3.17 FigureA4.17
FigureA5.17c FigureA5.17d
FigureA6.17c-1 FigureA6.17d-1

SQ-9 Offshore

FigureA1.18
FigureA2.18a FigureA2.18b
FigureA3.18 FigureA4.18
FigureA5.18c FigureA5.18d
FigureA6.18c-1 FigureA6.18d-1

SQ-Small Merged Data Set

FigureA1.20
FigureA2.20a FigureA2.20b
FigureA3.20 FigureA4.20
FigureA5.20a FigureA5.20b FigureA5.20c FigureA5.20d
FigureA6.20a FigureA6.20b FigureA6.20c FigureA6.20d

Appendix B: List of Figures

Merged: EW Profiles
Figure B1.1.2c.ps
Figure B1.1.2-5d.ps
Figure B1.1.4c.ps
Figure B1.1.5d.ps
Figure B1.1.2d.ps
Figure B1.1.3c.ps
Figure B1.1.4d.ps
Figure B1.1.2-5b.ps
Figure B1.1.3d.ps
Figure B1.1.5c.ps

Merged: NS Profiles
Figure B2.1.1-4d.ps
Figure B2.1.2d.ps
Figure B2.1.3d.ps
Figure B2.1.234d.ps
Figure B2.1.2-4c.ps
Figure B2.1.4c.ps
Figure B2.1.2c.ps
Figure B2.1.3c.ps
Figure B2.1.4d.ps

Merged: NE Profiles
Figure B3.1.23c.ps
Figure B3.1.2c.ps
Figure B3.1.3c.ps
Figure B3.1.23d.ps
Figure B3.1.2d.ps
Figure B3.1.3d.ps

Merged: NW Profiles
Figure B4.1.23c.ps
Figure B4.1.2c.ps
Figure B4.1.3c.ps
Figure B4.1.23d.ps
Figure B4.1.2d.ps
Figure B4.1.3d.ps

Merged: All Profiles
Figure B5.1.all-d.ps

Onshore & Merged: All Profiles
Figure B6.1.all-d.ps
Figure B6.1.all-h.ps

Onshore: NS Profiles
Figure B7.1.1a.ps and Figure B7.1.1b.ps

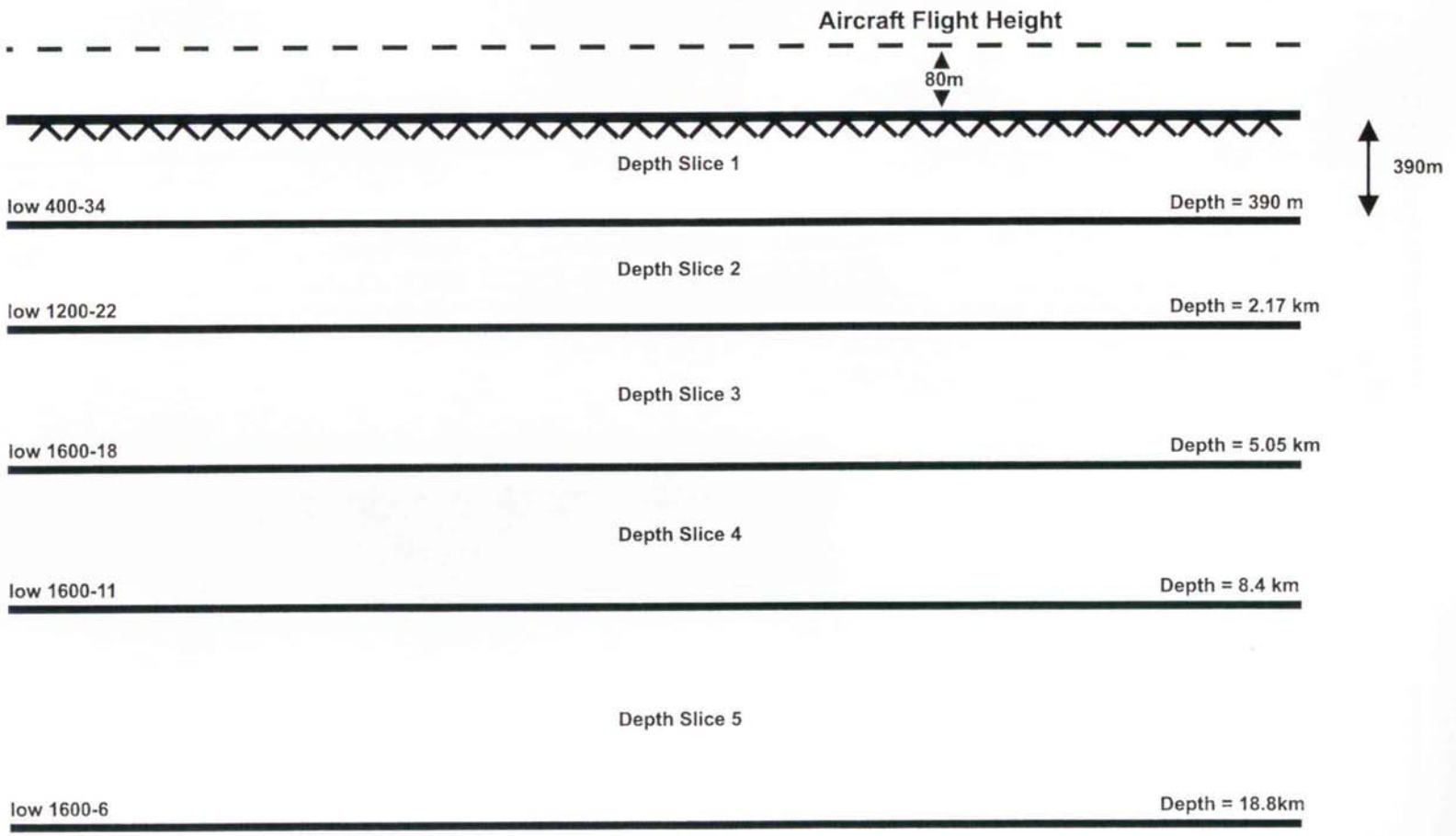

Figure 4b. Otway Basin, SQ-Large, Depth Slice Schematic

Figures 8a-c, Figures 9a-c, Figures 10a-c and **Figures 10_1a-10_1c** are plotted in 1:250,000 scale and are included in the **Enclosure** volume.